Current Optics and Photonics
Vol. 3, No. 3, June 2019, pp. 204-209

ISSN: 2508-7266(Print) / ISSN: 2508-7274(Online)
DOI: https://doi.org/10.3807/COPP.2019.3.3.204

Quadrature-detection-error Compensation in a Sinusoidally Modulated Optical Interferometer Using Digital Signal Processing

Jeong-hwan Hwang and Chang-Soo Park*

School of Electrical Engineering and Computer Science, Gwangju Institute of Science and Technology (GIST), Gwangju 61005, Korea

(Received March 28, 2019 : revised April 24, 2019 : accepted April 26, 2019)

In an optical interferometer that uses sinusoidal modulation and quadrature detection, the amplitude and offset of the interference signal vary with time, even without considering system noise. As a result, the circular Lissajous figure becomes elliptical, with wide lines. We propose and experimentally demonstrate a method for compensating quadrature detection error, based on digital signal processing to deal with scaling and fitting. In scaling, fluctuations in the amplitudes of in-phase and quadrature signals are compensated, and the scaled signals are fitted to a Lissajous unit circle. To do so, we scale the average fluctuation, remove the offset, and fit the ellipse to a unit circle. Our measurements of a target moving with uniform velocity show that we reduce quadrature detection error from 5 to 2 nanometers.

Keywords : Optical interferometer, Quadrature detection error compensation, Quadrature fringe measurement error, Quadrature detection
OCIS codes : (120.3940) Metrology; (120.3180) Interferometry; (120.0280) Remote sensing and sensors; (060.2370) fiber optics sensors

I. INTRODUCTION

Optical interferometers with quadrature detection have for decades been trusted for displacement measurements that require subnanometer resolution [1-6]. Especially, fiber-based optical interferometers using a telecom wavelength near 1550 nm and a sinusoidally modulated laser for quadrature detection are insensitive to mechanical stress, and benefit from commercialized, small optical components compared to conventional interferometers, which mostly use a 632-nm He-Ne laser and free-space bulk optics [3-6].

The primary performance limitation of fiber-based optical interferometers is quadrature detection error [3-13], which is caused by amplitude differences, dc offsets, and phase delays between the signals [12]. Furthermore, an in sinusoidally modulated optical interferometer, the signal amplitude varies with target movement [2]. Several methods have been introduced to reduce the quadrature detection error. While they showed good results under the condition that the error is fixed during measurement [8-13], in fact phase difference, offset, and gain could change with a moving target. Thus, a real-time compensation method is required.

In this paper, we propose and experimentally demonstrate a simple quadrature-detection-error-compensation method using digital signal processing. The quadrature detection error is mostly due to phase noise, and has the property of being recovered every cycle (period) of the phase signal. Therefore, we can largely reduce such error by compensating the amount of error every cycle for the target's motion.

II. PRINCIPLE OF OPERATION

A conventional sinusoidally modulated laser interferometer is shown in Fig. 1. The output signal generated by the interfering waves at the photodetector is expressed as [2]

*Corresponding author: csp@gist.ac.kr, ORCID 0000-0002-0130-6648
Color versions of one or more of the figures in this paper are available online.

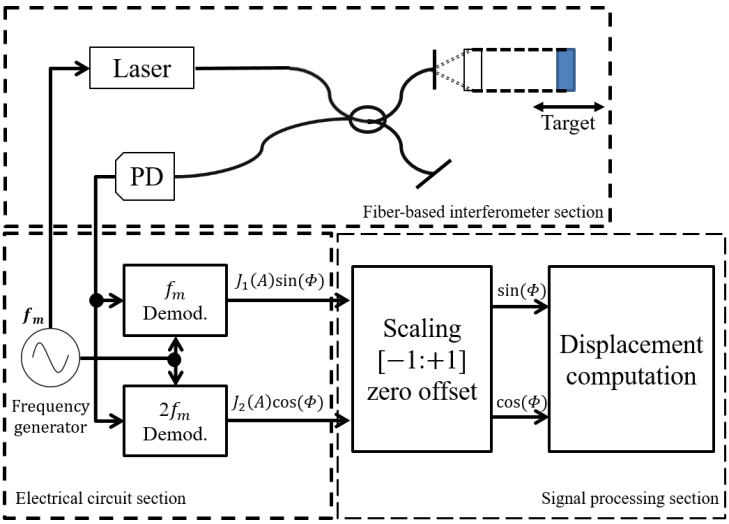

FIG. 1. Block diagram of a conventional optical interferometer using sinusoidal modulation.

$$I = \frac{I_0}{2}\left[1 + C\cos\left\{A\cos(2\pi f_m t) + \Phi\right\}\right], \tag{1}$$

where I_0 is the initial intensity, C is the interference contrast, f_m is the modulation frequency, Φ is the phase shift of the interfering signal (changing in time as the target moves, *i.e.* $\Phi(t)$; for simplicity, we use Φ instead of $\Phi(t)$), and A is the modulation depth, which is expressed as

$$A = -\left(\frac{4\pi npl}{\lambda_0^2}\right)\delta\lambda, \tag{2}$$

where $\delta\lambda$ is the wavelength shift due to sinusoidal modulation, λ_0 is the laser wavelength in free space, n is the refractive index, p is the folding order [3], and l is the path-length difference between the reference and sensing arms.

Eq. (1) can be expanded into

$$I = \frac{I_0}{2}(1 + CJ_0(A)\cos(\Phi)) - I_0 CJ_1(A)\sin(\Omega t)\sin(\Phi) + I_0 CJ_2(A)\cos(2\Omega t)\cos(\Phi) + \cdots, \tag{3}$$

where j_i is the Bessel function of the i^{th} kind, and Ω is the angular modulation frequency. After mixing this signal with $\sin(\Omega t)$ or $\cos(2\Omega t)$ and passing through a low-pass filter, we obtain two phase signals that have quadrature phase differences of

$$I_\Omega = -\frac{I_0 CJ_1(A)}{2}sin(\Phi), \tag{4}$$

$$I_{2\Omega} = -\frac{I_0 CJ_2(A)}{2}cos(\Phi). \tag{5}$$

From Eqs. (4) and (5) we derive the phase shift Φ to be

$$\Phi = \arctan\left(\frac{I_\Omega J_2(A)}{I_{2\Omega} J_1(A)}\right). \tag{6}$$

If we move the target from position x_1 to position x_2, the phase shift changes from Φ_1 to Φ_2. The displacement Δx (folding order $p = 2$) due to the phase change $\Delta\Phi = \Phi_2 - \Phi_1$ is calculated by

$$\Delta x = x_2 - x_1 = \frac{\lambda}{8\pi}\Delta\Phi. \tag{7}$$

However, for quadrature detection error, Eq. (4) and (5) become

$$I_\Omega^d = P_\Omega \sin(\Phi + \alpha_1) + O_\Omega + s_1, \tag{8}$$

$$I_{2\Omega}^d = P_{2\Omega}\cos(\Phi + \alpha_2) + O_{2\Omega} + s_2, \tag{9}$$

where P_Ω and $P_{2\Omega}$ are amplitudes, O_Ω and $O_{2\Omega}$ are dc offsets, s_1 and s_2 are the system noise terms, and α_1 and α_2 are the phase shifts caused by the quadrature detection error. In the presence of significant quadrature detection error, the Lissajous figure is distorted into an elliptical shape, as shown in Fig. 2(a). The amount of phase change is no longer $\Delta\Phi$, but becomes $\Delta\Phi' = \Delta\Phi + \Delta\beta$, where $\Delta\beta$ is the measurement error. The bottom of Fig. 2(a) shows the amplitudes of the in-phase (fundamental) and quadrature (second harmonic) signals in the time domain, with and without error. The phase changes $\Delta\Phi$ and $\Delta\Phi'$ and corresponding displacement values caused by the movement from point A to point B also differ visibly. Figure 2(b) shows the phase (displacement) error calculated from the phase signal, when compared with the ideal case. However, the increment in phase with error increases initially and then, even though the phase without error increases linearly with time.

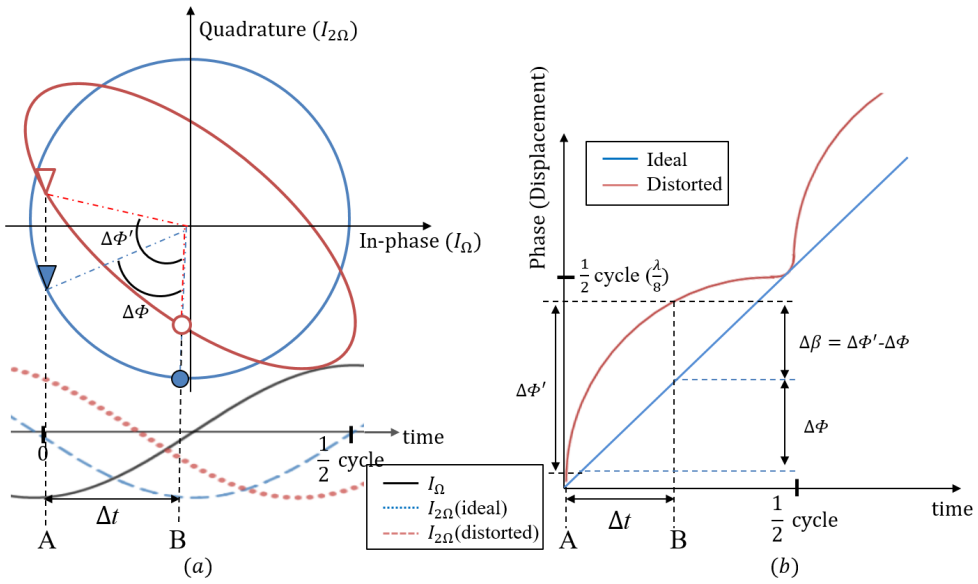

FIG. 2. Lissajous figures and phase shift (displacement) with and without quadrature detection error. Subplot (a) shows the phase error in the Lissajous figure (top) and the amplitudes of quadrature signals (bottom), and subplot (b) shows the phase error within one cycle.

To reduce this phase error, we propose a calibration method as follows: (1) scale the amplitude fluctuation in the phase signal so that the average amplitude fluctuation is zero, the maximum is +1, and the minimum is -1, and (2) fit the error ellipse to a unit circle using trigonometry. During this process we ignore system noise, including optical nonlinearity due to the high intensity of the light passing through the optical devices, and focus on the quadrature detection error.

After being scaled, the signal I^s is given by

$$I_{\Omega}^{s} = \sin(\Phi+\alpha_1), \tag{10}$$

$$I_{2\Omega}^{s} = \cos(\Phi+\alpha_2). \tag{11}$$

Applying the appropriate trigonometric formulas to I_{Ω}^{s} and $I_{2\Omega}^{s}$, we obtain Eqs. (12) and (13), which show a 90° phase difference between the two signals, and which simplify to

$$\begin{aligned} I_{\Omega}^{s}+I_{2\Omega}^{s} &= \sin(\Phi+\alpha_1)+\cos(\Phi+\alpha_2) \\ &= 2\cos(B_1)\sin(\Phi+B_2)2\cos(B_1)\sin(\Phi_c), \end{aligned} \tag{12}$$

$$\begin{aligned} I_{\Omega}^{s}-I_{2\Omega}^{s} &= \sin(\Phi+\alpha_1)-\cos(\Phi+\alpha_2) \\ &= 2\sin(B_1)\cos(\Phi+B_2)2\sin(B_1)\cos(\Phi_c), \end{aligned} \tag{13}$$

where B_1 is $\frac{\pi}{4}+\frac{\alpha_1-\alpha_2}{2}$, B_2 is $\frac{\pi}{4}+\frac{\alpha_1+\alpha_2}{2}$, and $\Phi_c = \Phi + B_2$. If we normalize the above signals, we obtain the Lissajous figure of a unit circle about Φ_c as

$$I_{\Omega}^{'} = \frac{I_{\Omega}^{s}+I_{2\Omega}^{s}}{2\cos(B_1)} = \sin(\Phi_c), \tag{14}$$

$$I_{2\Omega}^{'} = \frac{I_{\Omega}^{s}-I_{2\Omega}^{s}}{2\sin(B_1)} = \cos(\Phi_c). \tag{15}$$

Figure 3 shows the new process, after including our proposed modification. In the scaling section, "[-1: +1]" and "zero offset" denote the normalization process whereby we scale the amplitude to -1 and +1 with an average baseline of zero. In the proposed quadrature section, we fit the input signals $\sin(\Phi+\alpha_1)$ and $\cos(\Phi+\alpha_2)$ to $\sin(\Phi_c)$ and $\cos(\Phi_c)$.

We perform the signal processing using an analog-to-digital converter (ADC) and a buffer. For scaling, we sample the signals of Eqs. (10) and (11) and store them in the buffer as

$$I_{\Omega}^{d}[n] = I_{\Omega}^{d}(nT_s),\ I_{2\Omega}^{d}[n] = I_{2\Omega}^{d}(nT_s) \ \text{ for } \ n = 0, 1, 2 \cdots, N, \tag{16}$$

where T_s is the ADC's sampling period and N is the buffer size, which is capable of accommodating the data from at least one cycle. We scale the signals at the end of each cycle by applying Eq. (17) to the data stored in the buffer using

$$I_{i\Omega}^{s}[n] = \frac{2I_{i\Omega}^{d}[n]}{\max(I_{i\Omega}^{d}[n])-\min(I_{i\Omega}^{d}[n])} - avg(I_{i\Omega}^{d}[n]) \ \text{ for } \ n = 0, 1, 2 \cdots N \text{ and } i = 1, 2, \tag{17}$$

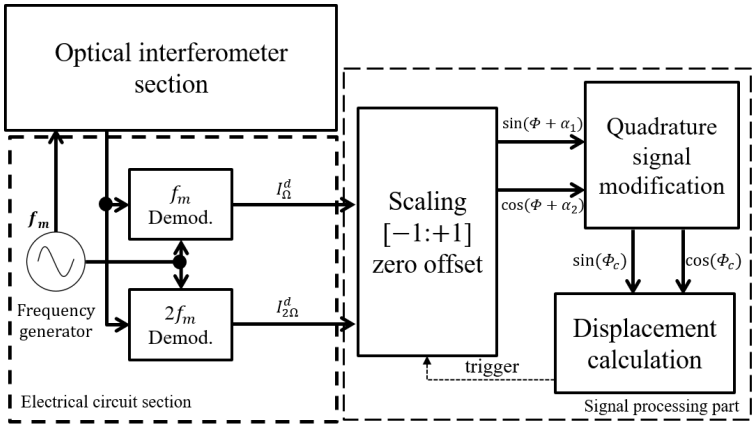

FIG. 3. Proposed signal-processing block diagram, with a step for quadrature signal modification.

where $\max(I^d_{i\Omega}[n])$ is the maximum of $I^d_{i\Omega}[n]$, $\min(I^d_{i\Omega}[n])$ is the minimum, and $avg(I^d_{i\Omega}[n])$ is the average value.

To convert the scaled data to a unit circle, we extend Eqs. (12) and (13) to

$$I^s_\Omega + I^s_{2\Omega} = 2\cos(B_1)\sin(\Phi[n]+B_2)2\cos(B_1)\sin(\Phi_c[n]), \tag{18}$$

$$I^s_\Omega - I^s_{2\Omega} = 2\sin(B_1)\cos(\Phi[n]+B_2)2\sin(B_1)\cos(\Phi_c[n]). \tag{19}$$

Eqs. (18) and (19) have a respective phase difference of 90°, and differ in amplitude. We normalize the in-phase and quadrature signals by taking

$$I'_\Omega[n] = \frac{I^s_\Omega + I^s_{2\Omega}}{2\cos(B_1)} = \sin(\Phi_c[n]), \tag{20}$$

$$I'_{2\Omega}[n] = \frac{I^s_\Omega - I^s_{2\Omega}}{2\sin(B_1)} = \cos(\Phi_c[n]). \tag{21}$$

Finally, we calculate the phase difference $\Delta\Phi_c[n]$ from the n^{th} to $(n+1)^{th}$ increments (see Fig. 4) using Eq. (6), as given by

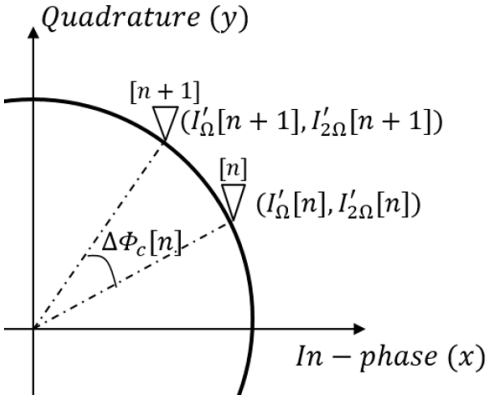

FIG. 4. Phase difference between the n^{th} and $(n+1)^{th}$ increments on the modified unit circle.

$$\begin{aligned}\Delta\Phi_c[n] &= \Phi_c[n+1] - \Phi_c[n] \\ &= \tan^{-1}\left(\frac{\tan\Phi_c[n+1] - \tan\Phi_c[n]}{1+\tan\Phi_c[n+1]\tan\Phi_c[n]}\right) \\ &= \tan^{-1}\left(\frac{I'_\Omega[n+1]I'_{2\Omega}[n] - I'_\Omega[n]I'_{2\Omega}[n+1]}{I'_\Omega[n]I'_\Omega[n+1] + I'_{2\Omega}[n]I'_{2\Omega}[n+1]}\right), \text{ for } n \\ &= n = 0,\ 1,\ 2\ \cdots\ N\end{aligned} \tag{22}$$

III. EXPERIMENTAL SETUP AND RESULTS

We configured our experiment as shown in Figs. 1 and 3 above. We used a laser diode (LD) with a center wavelength of 1554.94 nm and sinusoidally modulated at approximately 15 MHz. We adjusted the quadrature-signal amplitudes by controlling the depth of the sinusoidal LD modulation. We coupled the LD output into a fiber-based optical interferometer composed of an optical coupler, a collimator, and a target mirror mounted on a motorized stage. The interfered signal was converted into an electrical signal by a photodetector (PD) and demodulated into quadrature signals through a mixer and a low-pass filter. These signals were collected by a data acquisition (DAQ) system composed of two 12-bit ADCs with 1-kHz sampling speed (M2i.3021, Spectrum Ins.). Finally, the proposed compensation method was implemented using LabVIEW software for $n = 1024$. To obtain the Lissajous figures, we moved the target with uniform velocity. We did not attempt to stabilize our system, so that we could demonstrate the difference between our method and the method shown in Fig. 1.

Figure 5 shows the experimental results using our proposed method, as compared to the previous method that only uses scaling. As shown in Fig. 5(a), amplitude fluctuation of the signal including dc offset has disappeared through the proposed scaling method. In Fig. 5(b), I^s_Ω and $I^s_{2\Omega}$ with

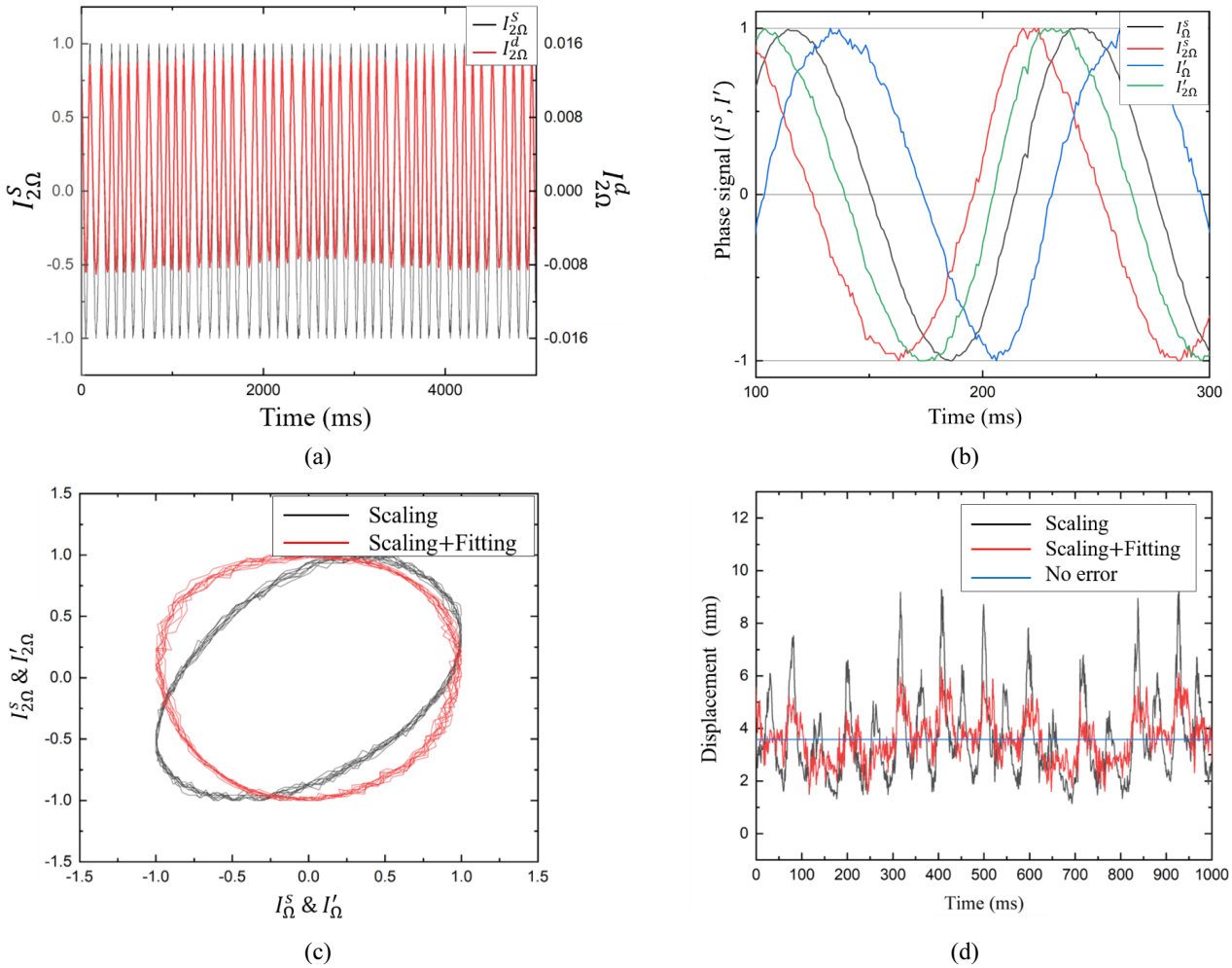

FIG. 5. Experimental results for the interferometer with scaling, scaling + fitting, and no error, showing (a) the signal before and after scaling for $I_{2\Omega,}$, (b) the phase signal, (c) the Lissajous figure, and (d) the displacement. Note that our method reduces the displacement error in (d) from 5 nm to 2 nm.

only scaling had a phase difference of about 45°, whereas $I_{\Omega}^{'}$ and $I_{2\Omega}^{'}$ had a phase difference of almost 90° after fitting; the corresponding Lissajous pattern of $I_{\Omega}^{'}$ and $I_{2\Omega}^{'}$ was much more circular in Fig. 5(c), since the phase difference was closer to 90°. Figure 5(d) shows the target displacement corrected using our proposed compensation, as compared to the previous method and to the ideal case. The displacement after both correction schemes still showed a small fluctuation, from about 5 nanometers using scaling only down to 2 nanometers using our proposed method of fitting plus scaling. We believe that the remaining fluctuation is most likely due to system noise, caused by high power modulation and external disturbances [2].

IV. CONCLUSION

We proposed a simple quadrature-detection-error-compensation method and demonstrated this approach experimentally. We normalized the in-phase and quadrature signals so that the maximum and minimum amplitudes were mapped to +1 and -1, followed by fitting the scaled signal to a unit circle through signal processing. Our experimental results showed that we reduced the quadrature detection error from 5 nanometers down to 2 nanometers, with the residual error likely caused by system noise from high power modulation.

ACKNOWLEDGMENT

This work was supported by GIST Research Institute (GRI) grant funded by the GIST in 2019.

REFERENCES

1. O. Sasaki and K. Takahashi, “Sinusoidal phase modulating interferometer using optical fibers for displacement

measurement," Appl. Opt. **27**, 4139-4142 (1988).
2. O. Sasaki, K. Takahashi, and T. Suzuki, "Sinusoidal phase modulating laser diode interferometer with a feedback control system to eliminate external disturbance," Opt. Eng. **29**, 1511-1515 (1990).
3. K. Thurner, F. P. Quacquarelli, P.-F. Braun, C. D. Savio, and K. Karrai, "Fiber-based distance sensing interferometry," Appl. Opt. **54**, 3051-3063 (2015).
4. K. Thurner, P.-F. Braun, and K. Karrai, "Absolute distance sensing by two laser optical interferometry," Rev. Sci. Instrum. **84**, 115002 (2013).
5. B. K. Nowakowski, D. T. Smith, and S. T. Smith, "Highly compact fiber Fabry-Perot interferometer: A new instrument design," Rev. Sci. Instrum. **87**, 115102 (2016).
6. J.-H. Hwang, S. Seon, and C.-S. Park, "Position estimation of sound source using three optical Mach-Zehnder Acoustic Sensor Array," Curr. Opt. Photon. **6**, 573-578 (2017).
7. M. Zhang, C. Ni, Y. Zhu, C. Hu, J. Hu, L. Wang, and S. Ding, "Sinusoidal phase-modulating laser diode interferometer for wide range displacement measurement," Appl. Opt. **56**, 5685-5691 (2017).
8. C.-M. Wu and C.-S. Su, "Nonlinearity in measurements of length by optical interferometry," Meas. Sci. Technol. **7**, 62-68 (1996).
9. N. Bobroff, "Residual errors in laser interferometry from air turbulence and nonlinearity," Appl. Opt. **26**, 2676-2682 (1987).
10. G. Dai, F. Pohelnz, H.-U. Danzebrink, K. Hasche, and G. Wilkening, "Improving the performance of interferometers in metrological scanning probe microscopes," Meas. Sci. Technol. **15**, 444-450 (2004).
11. Y.-C. Wang, L.-H. Shyu, C.-P. Chang, and E. Manske, "Signal interpolation method for quadrature phase-shifted Fabry-Perot interferometer," 58th Ilmenau Scientific Colloquium (2014).
12. P. L. M. Heydemann, "Determination and correction of quadrature fringe measurement errors in interferometers," Appl. Opt. **20**, 3382-3384 (1981).
13. K. A. Murphy, M. F. Gunther, A. M. Vengsarkar, and R. O. Claus, "Quadrature phase-shifted, extrinsic Fabry-Perot optical fiber sensors," Opt. Lett. **16**, 273-275 (1991).